

beam was formed by an electrostatic lens 4 on a Faraday cylinder 6. The energy was determined with the help of a magnetic analyzer and at energies less than 2 keV by the retarding potential method. The retarding potential was applied to a grid, positioned at the inlet to the Faraday cylinder. Figure 2 shows the dependence of the ion energy on the power introduced into the resonator at a frequency 1818 MHz ($W_{\max} = 15$ keV, $P_{\max} = 52$ kW). Figure 3 shows a similar dependence for the first variant of the source with gas injection in the range 0.01-0.68 cm³/h, and the absolute value of the power was not determined. The energies of the H⁺ and H₂⁺ ions are identical. Figure 4 shows the dependence of the ion current on the retarding potential, measured for the first variant of the source. The nonmonochromaticity of the beam was less than 10%. The maximum ion energy, obtained in the second variant, was 30 keV and the maximum current, conducted at a distance of 85 cm, was 3 mA. The dependence of the current on the gas flow rate was studied in detail for the first variant of the source. For ions with 2-keV energies, the dependence of the current on the gas flow rate for flow rates less than 0.1 cm³/h is linear. In this case, the use factor of the gas is close to 70%. Probably, the degree of ionization in the second variant is close to 100%, since the ion current at the closed end of the capillary (Fig. 5) is practically independent of the power for a constant gas flow rate.

LITERATURE CITED

1. M. D. Gabovich, Physics and Technology of Plasma Ion Sources [in Russian], Atomizdat, Moscow (1972).
2. V. L. Auslender, O. N. Brezhnev, and O. Ya. Savchenko, "Capillary uhf ion source," in: Proceedings of the Fifth All-Union Conf. on Charged Particle Accelerators, Vol. 1, Nauka, Moscow (1978).

DYNAMICS OF A PLASMA SHELL WITH AN OUTSIDE CURRENT

V. S. Komel'kov, A. P. Kuznetsov, V. V. Perebeinos,
A. S. Pleshanov, and M. T. Solomonov

UDC 533.9.07

The present article is an extension and development of the research of [1]. In this case the investigation was carried out on a more powerful experimental installation than in [1], while the numerical calculation method was considerably improved. Predicted variants of the plasma dispersion and acceleration beyond the accelerator electrodes on installations with still higher parameters, permitting a significant increase in the outside current, are theoretically analyzed.

1. Experiment

The plasma cluster was generated by a pulsed coaxial accelerator similar to that of [2]. The gas being accelerated and the atmosphere in which the acceleration and dispersion took place was hydrogen at a pressure of about $p_0 = 10^4$ Pa. Two capacitor batteries with a total capacitance of 72 μ F and a working voltage of 30 and 40 kV served as the accumulators. The method of repeated application of current [3] was used, so that by the moment the cluster emerged from the end of the accelerator the total current in the discharge reached 1.2 MA.

A diagram of the current supply and the design of the system of shaped electrodes of the plasma accelerated are shown in Fig. 1. The central electrode 1 consists of a tantalum rod 10 mm in diameter placed along the accelerator axis while the outer electrode 2 is a stainless steel cylinder, the inner diameter of which is 40 mm. The geometrical dimensions and shape of the electrodes are chosen so that ignition of the discharge took place not over the

Moscow. Translated from Zhurnal Prikladnoi Mekhaniki i Tekhnicheskoi Fiziki, No. 2, pp. 5-10, March-April, 1982. Original article submitted January 22, 1981.

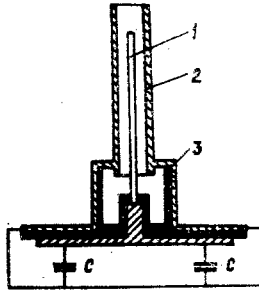


Fig. 1

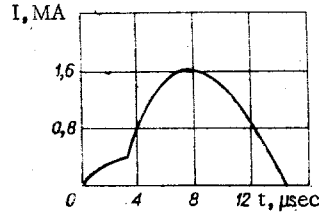


Fig. 2

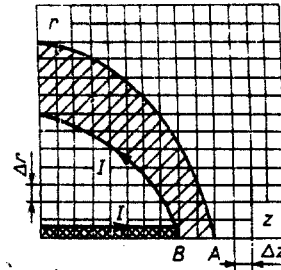


Fig. 3

surface of the insulator 3 but at some distance from it, which eliminated the involvement of the insulator material in the accelerated plasma, at least during the first quarter period of the discharge current.

A typical oscillogram of the current in an experiment is presented in Fig. 2, where the sharp bend corresponds to turning on the second battery.

The velocity of the plasma cluster was synchronized in time with the discharge current, which allowed us to determine the total current in the discharge at the moment the cluster emerged from the end of the accelerator. The shape and velocity of the plasma jet (obtained in different experiments) were determined from transverse photographic scans taken at different distances from the nozzle cut. The profile of the cluster was constructed from them. Unfortunately, the accuracy in determining the radial size of the latter was relatively low. We subsequently used experimental data only on the trajectory and velocity of the axial region of a cluster. These data, as in [2], helped in estimating the mass of the cluster and the current in it.

2. Calculation of Dispersion. Model and Method of Calculation

A plasma cluster moving beyond the limits of the nozzle consists of a "spouting pinch," which has been studied before [4, 5], which in the first phase includes both the plasma ejected from the accelerator and the plasma formed behind the shock wave front. The configuration of the jet, which consists of a hollow axisymmetric body, pertaining to a certain time is shown schematically in Fig. 3 (hatched region); the coordinate lines of the calculating grid and the current bridge (current filament) carrying the current I are also plotted here.

From the estimate $\delta/l \sim 1/\sqrt{\text{Re}_m}$ (see [6], for example), where δ is the thickness of the skin layer, l is the scale of length, and $\text{Re}_m = \mu\sigma vl$ is the magnetic Reynolds number (μ is the magnetic permeability, σ is the conductivity, and v is the scale of velocity), with the values $\mu \approx \mu_0 \approx 10^{-6}$ G/m, $\sigma \approx 10^4 - 10^6$ ($\Omega \cdot \text{m}$)⁻¹, $v \approx 10^4 - 10^5$ m/sec, and $l \approx 10^{-1}$ m we have $\text{Re}_m \approx 10 - 10^3$ and $\delta/l \approx 0.03 - 0.3$, so that the plasma can be taken as perfectly conducting, i.e., impenetrable for the magnetic field. We also adopt the usual assumptions about the quasineutrality of the plasma.

The system of hydrodynamic equations has the form

$$\begin{aligned} \frac{\partial u}{\partial t} + u \frac{\partial u}{\partial r} + v \frac{\partial u}{\partial z} + \frac{1}{\rho} \frac{\partial p}{\partial r} = 0, \quad \frac{\partial v}{\partial t} + u \frac{\partial v}{\partial r} + v \frac{\partial v}{\partial z} + \frac{1}{\rho} \frac{\partial p}{\partial z} = 0, \\ \frac{\partial \varepsilon}{\partial t} + u \frac{\partial \varepsilon}{\partial r} + v \frac{\partial \varepsilon}{\partial z} + \frac{p}{\rho} \left[\frac{1}{r} \frac{\partial}{\partial r} (ru) + \frac{\partial v}{\partial z} \right] = 0, \end{aligned} \quad (2.1)$$

where r and z are the radial and axial coordinates, respectively; u and v , radial and axial velocity components; ρ , density; p , pressure; ε , specific internal energy. To close system (2.1) we used tables of thermodynamic functions of hydrogen kindly presented by I. B. Rozhdestvenskii.

System (2.1) was solved using a modified method of particles in cells [7], which allowed us to get by without a continuity equation in (2.1), in particular. In the transport calculation the matter in each cell was modeled by a random distribution of from 100 to 1000 particles. The boundary of the cavity was traced cell by cell in accordance with the maximum (or minimum) coordinates of the particles which are in a given cell (or are transferred).

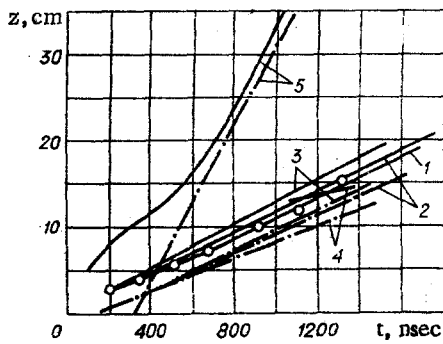


Fig. 4

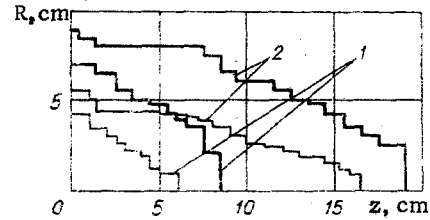


Fig. 5

Initial and Boundary Conditions. At the initial moment the plasma cluster was assumed to be a plasma disk compressed in a shock wave. The flow parameters behind the front of the shock wave compressing the hydrogen were determined from experimentally obtained data on the velocity of the shock front, $D_0 = 8 \cdot 10^4$ m/sec. In accordance with this we determined the following values: temperature $T_0 = 4 \cdot 10^4$ °K, $\rho_0 = 7 \cdot 10^{-2}$ kg/m³, $p_0 = 4.7 \cdot 10^7$ Pa, and $v_0 = 7 \cdot 10^4$ m/sec ($u_0 = 0$).

The boundary conditions were determined from the following considerations. The pressure of the atmosphere surrounding the cluster is 10^4 Pa and $\rho = 8.189 \cdot 10^{-3}$ kg/m³. A magnetic pressure determined by the current and the distance r from the axis acts inside the cavity, $P_m = \frac{1}{2} \mu_0 (I/2\pi r)^2$. Conditions of the "rigid wall" type were assigned at the coordinate surfaces $r = 0$ (the z axis) and $z = 0$ (the plane of the cut of the accelerator coaxial). Such a condition is quite natural for the z axis. It was also justified for the plane $z = 0$ by the fact that any noticeable outflow of plasma beyond this plane is absent in all the frames taken. In accordance with the amount of material ejected from the accelerator, the conditions of constancy of flow were maintained in the cells adjacent to the cut until the entire mass was expended. The formation of a cavity takes place starting with this moment. The pressure in the current bridge was determined from the condition of its equilibrium. According to the experimental data, the diameter of the current filament is 5 mm.

Results of Calculation and Comparison with Experiment. As in [1], the results of calculations of variants in which the entire discharge current I_0 and all the mass m_0 of gas contained in the accelerator were used as the determining quantities did not correspond to the experimental data. Variants in which $I = 0.3$ MA ($\sim 0.3I_0$) and the fraction of expelled mass was $(0.2-0.5)m_0$ yielded satisfactory agreement with experiment. Graphs of trajectories of the axial region of a cluster, obtained from experiment and by calculation, are presented in Fig. 4. Here the solid lines correspond to the outer boundary of the shell and the dash-dot lines to the inner boundary; curve 1 pertains to the experimental data. The calculations were made for two values of p_0 ($p_0 = 10^4$ Pa for curves 1-4; $p_0 = 10^3$ Pa for curves 5) and under three assumptions about the quantity dI/dt (see below). The satisfactory agreement between the quantities being compared allows us to speak rather confidently about the calculated parameters of a cluster, both as a whole and locally.

Figure 5 gives an idea of the configuration of the plasma shell at different times ($t = 0.72$ and 1.6 μ sec for lines 1 and 2, respectively; the heavy lines are the outer boundary of the shell and the thin lines are the inner boundary). The decrease in the velocity of the radial motion of the cavity boundary near the accelerator cut is clearly seen.

An analysis of the information obtained in the calculation allowed us to represent the picture of the dispersion as follows. The plug of compressed plasma which has shot out of the accelerator starts to expand intensely, creating a shock wave in the surrounding atmosphere. The magnetic field of the current, in acting as a piston, forms an expanding cavity; the radial motion of the cavity slows very rapidly owing to the quadratic radial decrease in magnetic pressure. On the other hand, the magnetic pressure remains constant in the axial region of the cluster and the flow here is determined by two factors: The magnetic piston strives to accelerate some mass of gas; this mass itself is formed in the complex interaction of the gas, already heated in the shock wave, which flows out into the axial region and the rarefaction wave drawing the gas toward the periphery of the cluster.

TABLE 1

P_0, Pa	10^3	10^4	10^5
I, MA			
0,3	$\alpha=9 \cdot 10^7$ $T=2 \cdot 10^6$ $k_T=4$ $v=3 \cdot 10^5$ $k_v=2$ $\rho=1,7 \cdot 10^{-3}$ $k_\rho=2$ $p=4 \cdot 10^2$ $k_p=1,3$	$\alpha=9 \cdot 10^6$ $T=5 \cdot 10^4$ $k_T=1$ $v=10^5$ $k_v=1,5$ $\rho=10^{-1}$ $k_\rho=10$ $p=4 \cdot 10^2$ $k_p=1$	
1	$\alpha=10^9$ $T=2 \cdot 10^7$ $k_T=3$ $v=1,3 \cdot 10^6$ $k_v=2$ $\rho=1,6 \cdot 10^{-3}$ $k_\rho=2$ $p=5 \cdot 10^3$ $k_p=1$	$\alpha=10^8$ $T=2,1 \cdot 10^6$ $k_T=3$ $v=3 \cdot 10^5$ $k_v=2$ $\rho=2 \cdot 10^{-2}$ $k_\rho=2,5$ $p=4,5 \cdot 10^3$ $k_p=1$	$\alpha=10^7$ $T=3 \cdot 10^4$ $k_T=1$ $v=10^5$ $k_v=1,6$ $\rho=6 \cdot 10^{-1}$ $k_\rho=9$ $p=3 \cdot 10^3$ $k_p=1$
2		$\alpha=4 \cdot 10^8$ $T=8 \cdot 10^6$ $k_T=2,6$ $v=7,8 \cdot 10^5$ $k_v=2$ $\rho=1,5 \cdot 10^{-2}$ $k_\rho=2$ $p=2 \cdot 10^4$ $k_p=1$	$\alpha=4 \cdot 10^7$ $T=5 \cdot 10^6$ $k_T=2,5$ $v=2,3 \cdot 10^5$ $k_v=2$ $\rho=2,4 \cdot 10^{-1}$ $k_\rho=3$ $p=2 \cdot 10^4$ $k_p=1$

The effect of an increase in the velocity of the axial region of the cluster near the accelerator cut is explained by the maximum value of the magnetic pressure in this region which acts on an approximately constant mass of the axial region (the gas flowing out through the shock front is transported toward the periphery of the cluster by the rarefaction wave). The acceleration of the axial region may be less inside the coaxial owing to the increase in the mass of this region as the shock wave advances (the lateral rarefaction wave is less intense owing to the unclearly expressed departure from a one-dimensional flow pattern). The following facts are characteristic for the variant being calculated: a) the motion of the axial region takes place with a constant velocity, exceeding D_0 by 1.5-2 times, starting with a certain moment; b) the radial motion of the cluster takes place in such a way that the radial velocity of each point of the outer and inner contours passes through a maximum, equal to $3,5 \cdot 10^4$ m/sec for points of the inner contour; c) the inner cavity undergoes slight oscillations about some average position; d) the temperature of the cluster near the outer boundary is practically constant over the contour (except for the axial region), and starting with $t \approx 200$ nsec it does not depend on time and is 10^4 °K; e) the flow parameters in the axial region arrive at stationary values, with the temperature here reaching $5 \cdot 10^4$ °K, the density 10^{-1} kg/m³ (a compression ratio of about 10), and the pressure $4 \cdot 10^7$ Pa; f) starting with a certain moment, energy "pumping" into the cluster proceeds at a constant rate.

Besides the calculation variant with the parameters of the experiment, predictive calculations were made in which the values of the current I and the initial gas density ρ_0 were varied. The need to make such calculations was dictated by the fact that the phenomenon of the acceleration of plasma clusters and their dispersion are attracting more and more attention, while the calculation method developed and the mathematical model of dispersion allow us to obtain sufficiently reliable data.

Before turning to a review of the results of these calculations, we should say a few words about the choice of the parameters of plasma flow in the accelerator. Remember that experimental data were available (and only on the velocity of the plasma front) for the case in which the effective current was estimated as 0.3 MA while the hydrogen density in the accelerator corresponded to a pressure of about 10^4 Pa. The pressure p behind the front was determined from data on the velocity D of the front. We found the value of the radius (r_{ef}) at which the value of I adopted as the effective current created a magnetic pressure p_m equal to p . For all the predictive variants the parameters of the shock wave inside the accelerator were determined on the basis of the values of the effective current and gas density adopted in the variant, using r_{ef} determined, as stipulated above, for the variant in agreement with experiment. Such a system for determining the parameters of the shock wave assured the correctness of the procedure for comparing the calculated results of all the variants. It is convenient to characterize the variants by the parameter $\alpha = I^2/p_0$ ($10^7 < \alpha < 10^9$ in the calculated variants).

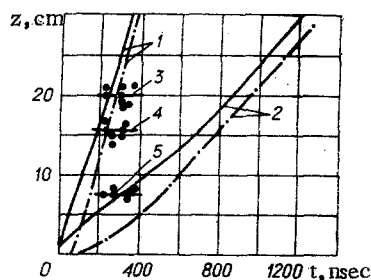


Fig. 6

Table 1 gives an idea of some results of the calculation of such variants. The variant with $I = 0.3$ MA and $p_0 = 10^5$ Pa held no interest from the aspect of attaining extremal values of T or ρ , and therefore it was not calculated. The variant with $I = 2$ MA and $p_0 = 10^3$ Pa evidently could predetermine very high flow parameters, but it would require allowance for radiative transfer and so it too was not calculated. As for the remaining variants, the absence of the allowance for radiative transfer in them is still permissible, although the results obtained are somewhat overstated. A number of general tendencies and dependences should be noted for all the variants: The motion of the axial region arrives at a steady state; the arrival of T and ρ at steady values in the axial region is delayed, with the gas being intensely heated and expanding; energy "pumping" into the cluster takes place at a constant rate.

An analysis of the table reveals the asymptotic behavior (as $\alpha \rightarrow \infty$) of a number of important characteristics of the axial region of flow: $k_T = T/T_{sw}$, $k_v = v/v_{sw}$, $k_p = p/p_{sw}$, $k_\rho = \rho/\rho_0$ (T , v , p , and ρ are the temperature, axial velocity, pressure, and density, respectively, in the axial region upon arrival at a steady state), while the index sw indicates that the values of the respective quantities are determined for the shock wave formed in the coaxial of the accelerator. Figures 4 and 6 are an illustration of this. The trajectories of motion of the outer and inner points of a plasma cluster (points A and B, respectively, in Fig. 3) located at its axis are shown in Fig. 4. In Fig. 6 we show the analogous dependences for two variants in which the current I was taken as 2 MA while the pressure p_0 took values of 10^4 Pa (curves 1) and 10^5 Pa (curves 2). Besides the trajectories, the time dependences of the quantities, p , ρ , and T (curves 3-5, respectively) are shown in Fig. 6 for the variant with $p_0 = 10^4$ Pa.

The arrival of all the flow characteristics at the steady state is well seen. The dots shown in these dependences illustrate the scatter of the calculated results, caused by the fact that the Lagrangian coordinates of particles in a cell are random numbers. The scatter of the results is small; not more than 7.5% for p , not more than 10% for ρ , and not more than 6% for T . The question of the influence of the time variation of the current on the parameters of motion of a plasma cluster is of definite interest. Two cases could be fully realistic here: the current decreases as the induction in the accelerator-cluster system increases (the length of the current filament increases and the radius of the cavity varies); the current increases (as a result of connecting the new battery). An estimate of the decrease in current as a result of the change in inductance showed that for the variant with $I = 0.3$ MA and $p_0 = 10^4$ Pa this decrease is no more than 50% over a characteristic time of 1 μ sec. Variants in which the current varied with time as $I = I_0(1 + kt)$ ($k = \pm 0.5 \cdot 10^6$) were calculated. The trajectories of points A and B for both values of p_0 are presented in Fig. 4. Here curves 2 correspond to $k = 0$, curves 3 to $k = 0.5 \cdot 10^6$, and curves 4 to $k = -0.5 \cdot 10^6$. As seen from a comparison with the corresponding variant with $I = 0.3$ MA and $p_0 = 10^4$ Pa, the allowance for variation of the current led to slight corrections to the trajectories and all the other flow parameters.

This investigation allowed us to obtain quantitative characteristics of the flow of a hydrogen plasma and to reveal a number of important qualitative relationships. The results of the predictive calculations indicate the fully realistic possibility of obtaining a dense high-temperature plasma in the continuous medium beyond the end of the accelerator. In this case the latter fills the function of an "accentuator," making it possible to increase the discharge current to the highest possible values during the motion of the plasma in it. If

one has in mind modes with high values of the discharge current, then estimates of the velocity of the front and the flow velocity can be obtained by multiplying by two the values of the respective quantities measured in the accelerator coaxial. The temperature is estimated by multiplying the plasma temperature behind the shock wave in the accelerator by a number close to three, while estimating the density comes down to multiplying by two the value of the gas density in the accelerator before the discharge. The pressure remains practically what it was in the gas compressed by the shock wave inside the accelerator, with the condition that it is fully engulfed.

LITERATURE CITED

1. V. S. Komel'kov, A. P. Kuznetsov, et al., "Dispersion of a plasma current shell," *Zh. Prikl. Mekh. Tekh. Fiz.*, No. 5 (1978).
2. V. S. Komel'kov and V. I. Modzolevskii, "Formation of a plasma jet in air at atmospheric pressure," *Zh. Tekh. Fiz.*, 41, No. 5 (1971).
3. V. S. Komel'kov and V. I. Modzolevskii, "Plasma acceleration by the repeated application of current," in: *Fourth All-Union Conference on Plasma Accelerators and Ion Injectors, Summaries of Reports [in Russian]*, Moscow (1978).
4. V. S. Komel'kov, "Motion of the plasma of a powerful discharge in the magnetic field of its own current," in: *Nuclear Physics, Proceedings of the Second International Conference on the Peaceful Use of Atomic Energy [in Russian]*, Vol. 1, Moscow (1959).
5. V. I. Vasil'ev, V. S. Komel'kov, et al., "A stable dynamic current filament," *Zh. Tekh. Fiz.*, 30, No. 7 (1960).
6. L. D. Landau and E. M. Lifshits, *Electrodynamics of Continuous Media*, Pergamon (1960).
7. A. P. Kuznetsov and A. S. Pleshanov, "A numerical investigation of Prandtl-Meyer MHD flow," *Magn. Gidrodin.*, No. 4 (1976).

CHARACTERISTICS OF CO₂ LASER MEDIA WITH A HIGH PUMPING LEVEL

V. V. Osipov, V. V. Savin, and V. A. Tel'nov

UDC 533.9.543.42

The promise of achieving high specific power levels and efficiencies has stimulated study of continuous CO₂ lasers. Increase in laser radiation power requires an increase in pump power and pressure of the operating medium, which, as a rule, is accompanied by localization of the discharge and termination of energy supply into the gas. The discharge stability limit is determined to a significant degree by the excitation methods used. The best success has been achieved with use of electrical ionization for excitation in CO₂ lasers, with discharge power levels of 10 W/cm³ being achieved [1].

Significantly higher discharge powers have been obtained in experiments on studies of volume discharges for CO₂ lasers with use of denser electron beams [2]. However, an increase in power level of external ionizers in continuous CO₂ lasers is prevented by heating and destruction of the thin metal foils which separate the gas container and the accelerator vacuum diode [3]. Introduction of electron beams into the operating medium through gasdynamic windows [4] has not yet been used widely because of the complexity of the construction required to produce the large pressure differential between the gas container and accelerator operating volume.

Use of a combined discharge [5-7] is a more promising means of achieving these goals. In this case the major fraction of the energy is introduced into the gas with a lengthy non-independent discharge in the plasma recombination decay stage, and creation of the charged particle concentration required to maintain the current in the operating volume is accomplished by a brief independent discharge. The major difficulty in exciting gaseous media in this manner at a high power level is the necessity of using means of decoupling the electrical circuits of the independent and dependent discharges which will not limit the current of the dependent discharge.

Tomsk. Translated from *Zhurnal Prikladnoi Mekhaniki i Tekhnicheskoi Fiziki*, No. 2, pp. 10-17, March-April, 1982. Original article submitted February 2, 1981.